We are IntechOpen, the world's leading publisher of Open Access books
Built by scientists, for scientists

6,900
Open access books available

185,000
International authors and editors

200M
Downloads

154
Countries delivered to

Our authors are among the

TOP 1%
most cited scientists

12.2%
Contributors from top 500 universities

CLARIVATE ANALYTICS
BOOK CITATION INDEX
INDEXED

WEB OF SCIENCE™

Selection of our books indexed in the Book Citation Index
in Web of Science™ Core Collection (BKCI)

Interested in publishing with us?
Contact book.department@intechopen.com

Energy-Efficient Walking for Biped Robot Using Self-Excited Mechanism and Optimal Trajectory Planning

Qingjiu Huang & Kyosuke Ono
Tokyo Institute of Technoligy, Japan

1. Introduction

Recently, a lot of researches which aim at realization of dynamic biped walking are being performed. There is Honda's ASIMO as a representative of researches of humanoid robots. ASIMO has joints of many degrees of freedom that are near to a human being, high environment adaptability and robustness, and can do various performances. However, it needs many sensors, complicated control, and walks with bending a knee joint to keep the position of a centre of gravity constant. Therefore, it walks unnaturally and consumes much energy.

On the other hand, McGeer performed the research of passive dynamic walking from the aspect of that it is natural motion in a gravitational field (McGeer, T., 1990). This robot which could go down incline only using potential energy was developed and realized the energy-efficient walking. However, it needs incline, and its applied range is small because it has no actuator. Therefore, the researches that aimed at energy-efficient biped walking on level ground have been performed. S.H.Collins exploited the robot which had actuators at only ankles (Collins, S. H. & Ruina A., 2005). M.Wisse exploited the robot which used pneumatic actuators (Wisse, M. & Frankenhuyzen, J. van, 2003). Ono exploited the self-excitation drive type robot which had an actuator only at hip joint (Ono, K. et al, 2001); (Ono, K. et al, 2004); (Kaneko, Y. & Ono K., 2006). And then, Osuka and Asano performed the level ground walking from a point of view to mechanical energy for joints which is the same with the energy consumed of passiveness walk (Osuka, K. et al, 2004); (Asano, F. et al, 2004). These biped robot's studies used the technique of the passive dynamic walking which used inertia and gravity positively by decreasing the number of actuators as much as possible. However, in order to adapt the unknown ground, the biped robot needs actuators to improve the environment adaptability and robustness. Here, Ono proposed the optimal trajectory planning method based on a function approximation method to realize an energy-efficient walking of the biped robot with actuators similar to a passive dynamic walking (Imadu, A. & Ono, K. 1998); (Ono, K. & Liu, R., 2001); (Ono, K. & Liu, R., 2002); (Peng, C. & Ono K., 2003). Furthermore, Huang and Hase verified the optimal trajectory planning method for energy-efficient biped walking by experiment, and proposed the inequality state constraint to obtain better solution which is desirable posture in the intermediate time of the walking period (Hase, T. & Huang, Q., 2005); (Huang, Q. & Hase, T., 2006); (Hase, T., et al., 2006).

In this chapter, we introduce the newest researches on energy-efficient walking of the biped robot for level ground form two viewpoints, one is semi-passive dynamic walking with only hip actuator using self-excited mechanism, another is active walking with actuators using optimal trajectory planning.

The chapter is organized as follows. In section 2, the self-excited walking of a four-link biped robot and the self-excitation control algorithm enables the robot to walk on level ground by numerical simulation and experiment will be introduced. In section 3, we aim at realizing an energy-efficient walking of the four-link biped robot with actuators similar to a passive dynamic walking. An optimal trajectory planning method based on a function approximation method applied to a biped walking robot will be shown. And then, we use the inequality state constraint in the intermediate time and restrict the range of joint angles. In this way, a better solution which is desirable posture in the intermediate time can be obtained. Furthermore, in section 4, with "Specific Cost", we show that the biped walking with the above two methods have more efficient energy than the other methods which use geared motors. Finally, the conclusions will be presented in section 5.

2. Self-Excited Walking for Biped Mechanism

In this section, we introduce a study on the self-excited walking of a four-link biped mechanism that proposed by Ono (Ono, K. et al, 2001). And then, we show that the self-excitation control enables the three-degree-of-freedom planar biped model to walk on level ground by numerical simulation. From the parameter study, it was found that stable walking locomotion is possible over a wide range of feedback gain and link parameter values and that the walking period is almost independent of the feedback gain. Various characteristics of the self-excited walking of a biped mechanism were examined in relation to leg length and length and mass ratios of the shank. Next, a biped mechanism was manufactured similar to the analytical model. After parameter modification the authors demonstrated that the biped robot can perform natural dynamic walking on a plane with a 0.8 degree inclination. The simulated results also agree with the experimental walking locomotion.

2.1 Analytical Model of Biped Walking Robot and Kinetic Process

2.1.1 Features of Biped Locomotion and Possibility of Its Self-Excitation

Fig.1 shows a biped mechanism to be treated in this study. Here we focus only on the biped locomotion in the sagittal plane. The biped mechanism does not have an upper body and consists of only two legs that are connected in a series at the hip joint through a motor. Each leg has a thigh and a shank connected at a passive knee joint that has a knee stopper. By the knee stopper, an angle of the knee rotation is restricted like the human knee. The legs have no feet, and the tip of the shank has a small roundness. The objective of this study is to make the biped mechanism perform its inherent natural walking locomotion on level ground not by gravitational force but by active energy through the hip motor.

The necessary conditions for the biped mechanism to be able to walk on level ground are as follows: (1) The inverted pendulum motion for the support leg must synchronize with the swing leg motion. (2) The swing leg should bend so that the tip does not touch the ground. (3) The dissipated energy of the mechanism through collisions at the knee and the ground, as well as friction at joints, should be supplied by the motor. (4) The knee of the support leg

should not be bent by the internal force of the knee stopper. (5) The synchronized motion between the inverted pendulum motion of the support leg and the two-DOF pendulum motion of the swing leg, as well as the balance of the input and output energy, should have stable characteristics against small deviations from the synchronized motion.
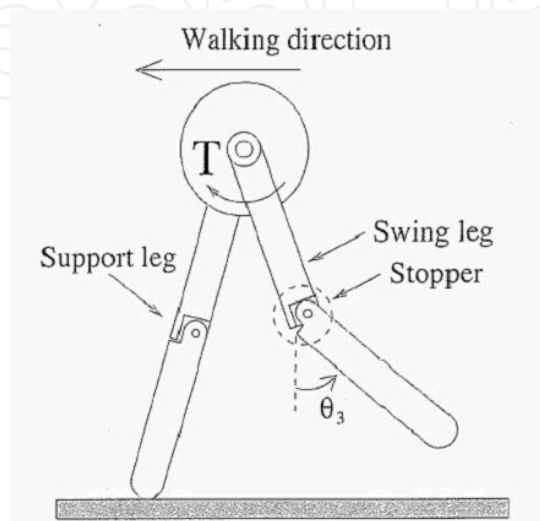

Fig.1. Three-degree-of freedom walking mechanism on a sagittal plane (Ono, K. et al, 2001)

First we pay attention to the swing leg and try to generate a swing leg motion that can satisfy the necessary conditions (2) and (3) by applying the self-excitation control to the swing leg motion. Ono and Okada (Ono, K. & Okada, T., 1994) have already investigated two kinds of self-excitation control of two-DOF vibration systems and showed that the Van der Pol-type self-excitation can evoke natural modes of the original passive system, while the asymmetrical stiffness matrix type can excite the anti-resonance mode that has a phase shift of about 90 degrees between input and output positions.

The two-DOF pendulum of a swing leg has the first-order mode with an in-phase at each joint and the second-order mode with an out-of-phase at each joint. Thus, it will be impossible to generate a walking gait by applying the Van der Pol-type self-excitation. In contrast, by means of the negative feedback from the shank joint angle θ_3 to the input torque T at the thing joint, the system's stiffness matrix becomes asymmetrical. Thus, the swing motion would change so that the shank motion delays at about 90 degrees from the thigh motion. Through this feedback, it is also expected that the kinetic energy of the swing leg increases and that the reaction torque (=T) will make the support leg rotate in the forward direction in a region where $\theta_3 > 0$. The self-excitation of the swing leg based on the asymmetrical matrix is explained in detail below.

2.1.2 Self-Excitation of the Swing Leg

Fig.2 depicts the two-DOF swing leg model whose first joint is stationary. To make Fig..2 compatible with Fig.3 (b), the upper and lower links are termed the second and third links, respectively. To generate a swing motion like a swing leg, only the second joint is driven by the torque T2, which is given by the negative position feedback of the form
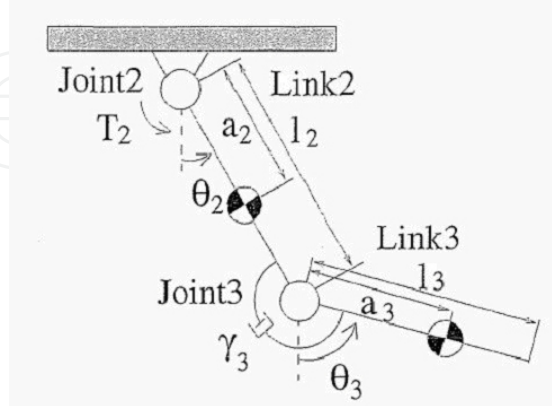
$$T_2 = -k\theta_3 .$$ (1)

Fig.2. Analytical model of two-degree-of-freedom swing leg (Ono, K. et al, 2001)

From the fundamental study of the asymmetrical stiffness matrix-type self-excitation (Ono, K. & Okada, T., 1994), it is known that damping plays an important role in inducing the self-excited motion. Thus, the viscous rotary damper with coefficient γ_3 is applied to joint 3.

Taking Eq. (1) into account, the equation of motion for the two-DOF pendulum system is written as

$$
\begin{bmatrix} I_2 + m_2 a_2^2 + m_3 l_2^2 & m_3 a_3 l_2 \cos(\theta_3 - \theta_2) \\ m_3 a_3 l_2 \cos(\theta_3 - \theta_2) & I_3 + m_3 a_3^2 \end{bmatrix} \begin{bmatrix} \ddot{\theta}_2 \\ \ddot{\theta}_3 \end{bmatrix}
$$
$$
+ \begin{bmatrix} \gamma_3 & -m_3 a_3 l_2 \sin(\theta_3 - \theta_2)\dot{\theta}_3 - \gamma_3 \\ m_3 a_3 l_2 \sin(\theta_3 - \theta_2)\dot{\theta}_2 - \gamma_3 & \gamma_3 \end{bmatrix} \begin{bmatrix} \dot{\theta}_2 \\ \dot{\theta}_3 \end{bmatrix}
$$
$$
+ \begin{bmatrix} (m_2 a_2 + m_3 l_2) g \sin\theta_2 / \theta_2 & k \\ 0 & m_3 a_3 g \sin\theta_3 / \theta_3 \end{bmatrix} \begin{bmatrix} \theta_2 \\ \theta_3 \end{bmatrix} = 0.
$$ (2)

We note from Eq. (2) that the stiffness matrix of the system becomes asymmetrical because of the feedback gain k.

To examine the value of k to excite a swing leg motion autonomously and the natural frequency and mode at the threshold, Eq. (2) is linearized about $\theta_2 = \theta_3 = 0$. The linearized equation of motion becomes

$$
\begin{bmatrix} I_2 + m_2 a_2^2 + m_3 l_2^2 & m_3 a_3 l_2 \\ m_3 a_3 l_2 & I_3 + m_3 a_3^2 \end{bmatrix} \begin{bmatrix} \ddot{\theta}_2 \\ \ddot{\theta}_3 \end{bmatrix} + \begin{bmatrix} \gamma_3 & -\gamma_3 \\ -\gamma_3 & \gamma_3 \end{bmatrix} \begin{bmatrix} \dot{\theta}_2 \\ \dot{\theta}_3 \end{bmatrix} + \begin{bmatrix} (m_2 a_2 + m_3 l_2) g & k \\ 0 & m_3 a_3 g \end{bmatrix} \begin{bmatrix} \theta_2 \\ \theta_3 \end{bmatrix} = 0.
$$ (3)

Putting $\theta_2 = \Theta_2 e^{\lambda t}$ and $\theta_3 = \Theta_3 e^{\lambda t}$ into Eq. (3), we have

$$
\begin{bmatrix} a_{11}\lambda^2 + \gamma_3 \lambda + k_{11} & a_{12}\lambda^2 - \gamma_3 \lambda + k \\ a_{21}\lambda^2 - \gamma_3 \lambda & a_{22}\lambda^2 + \gamma_3 \lambda + k_{22} \end{bmatrix} \begin{bmatrix} \Theta_2 \\ \Theta_3 \end{bmatrix} = 0.
$$ (4)

Where $a_{11} = I_2 + m_2 a_2^2 + m_3 a_2^2$, $a_{12} = a_{21} = m_3 a_3 I_2$, $a_{22} = I_3 + m_3 a_3^2$, $k_{11} = (m_2 a_2 + m_3 I_2)g$,
$k_{22} = m_2 a_3 g$.

From the condition that the determinant in Eq. (4) is zero, we can obtain the characteristic equation of the linearized system of the form

$$A_0 \lambda^4 + A_1 \lambda^3 + A_2 \lambda^2 + A_3 \lambda + A_4 = 0. \tag{5}$$

As k increases, one of the eigenvalues becomes unstable. At the boundary, λ becomes an imaginary number. Thus, putting $\lambda = \omega i$ into Eq. (5), we can get the critical k value and the natural frequency at the inst ability threshold.

Here we assume that both links are a uniform bar whose length is 0.4 m ($= l_2 = l_3$), and the mass is 2 kg ($= m_2 = m_3$). For these link parameters, one of the natural modes becomes unstable when k > 1.43 or k < -3.14. The natural frequency of the unstable swing motion at k= 1.43 is 0.71 Hz, whereas that at k = -3.14 is 0.61 Hz. If the damping does not exist at joint 3, one of the natural modes becomes unstable when 30.4 > K > 6.3. Note that the damping coefficient γ_3 , however small it might be, can significantly reduce the critical k value. Strangely enough, the magnitude of the damping coefficient γ_3 does not change the critical k value and the natural frequency at the threshold. However, the damping coefficient value slightly influences the natural mode of the unstable vibration. By putting the natural frequency and k value into Eq. (4) , we found a swing motion such that the lower link delays from the upper link are excited when k ≥ 1.43. The magnitude and phase of Θ_2 / Θ_3 are 0.60 and 8.89 degrees, respectively, when γ_3 = 0.15 Nms/rad. As the unstable vibration grows in magnitude and approaches a limit cycle, the phase of the Θ_2 / Θ_3 tends to be 90 degrees (Ono, K. & Okada, T., 1994).

2.2 Analytical Model of Biped Locomotion and Basic Equations

The next question is whether the biped mechanism, which combines the two-DOF swing leg discussed in Section 2.1 and the single-DOF support leg, can generate a biped locomotion that satisfies the conditions (1), (4), and (5). Since it is difficult to derive this solution analytically, we numerically show that the nonlinear biped system excited by the asymmetrical feedback exhibits a stable biped locomotion that satisfies the three conditions as a limit cycle of the system.

Fig.3 (a) shows the representative postures of a biped mechanism during half of the period of biped locomotion. From an aspect of the difference of the basic equation, one step process can be divided into two phases: (1) from the start of the swing leg motion to the collision at the knee (the first phase) and (2) from the knee collision to the touchdown of the straight swing leg (the second phase). We assume that the change of the support leg to the swing leg occurs instantly and that the end of the second phase is the beginning of the first phase. The self-excitation feedback of (1) is applied only during the first phase. We assume that the support leg is kept straight because of internal reaction torque at the knee for simplifying the forward dynamic simulation. The validity of this assumption will be examined later.

Under the assumption of a straight support leg, the analytical model during the first phase is represented as a three-DOF link system, as shown in Fig.3 (b). Viscous damping is applied to the knee joint of the swing leg. The equation of motion in this system during the first phase is written as

$$\begin{bmatrix} M_{11} & M_{12} & M_{13} \\ & M_{22} & M_{23} \\ sym & & M_{33} \end{bmatrix} \begin{bmatrix} \ddot{\theta}_1 \\ \ddot{\theta}_2 \\ \ddot{\theta}_3 \end{bmatrix} \tag{6}$$

Where the elements M_{ij}, C_{ij}, and K_i of the matrices are shown in Appendix A. T2 is feedback input torque given by Eq. (1).
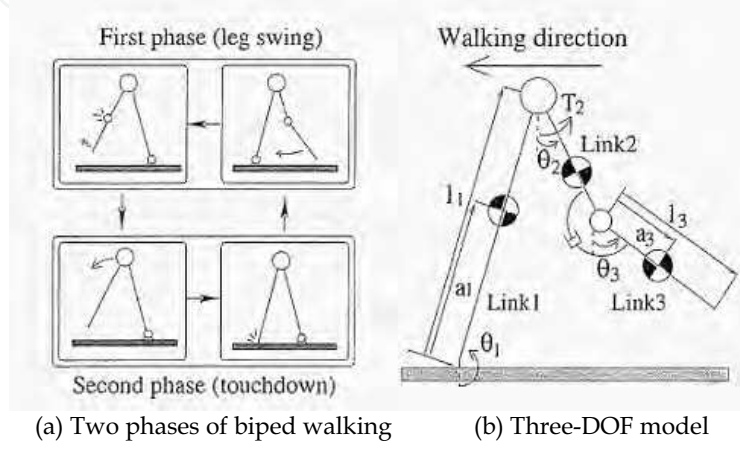

(a) Two phases of biped walking   (b) Three-DOF model

Fig.3. Analytical model of three-degree-of-freedom walking mechanism (Ono, K. et al, 2001)

When the shank becomes straight in line with the thigh at the end of the first phase, it is assumed that the knee collision occurs plastically. From the assumption of conservation of momentum and angular momentum before and after the knee collision, angular velocities after the knee collision are calculated from the condition $\dot{\theta}_2^+ = \dot{\theta}_3^+$ and the equation of the form

$$\begin{bmatrix} \dot{\theta}_1^+ \\ \dot{\theta}_2^+ \\ \dot{\theta}_3^+ \end{bmatrix} = [M]^{-1} \begin{bmatrix} f_1\left(\theta_1, \dot{\theta}_1^-\right) \\ f_2\left(\theta_2, \dot{\theta}_2^-\right) - \tau \\ f_3\left(\theta_3, \dot{\theta}_3^-\right) + \tau \end{bmatrix}, \tag{7}$$

Where the elements of the matrix [M] are the same as M_{ij} in Eq. (6). f_1, f_2, and f_3 are presented in Appendix B. τ is the moment impulse at the knee.

During the second phase, the biped system can be regarded as a two-DOF link system. Thus, the basic equation becomes

$$\begin{bmatrix} I + m_1 a_1^2 + m_2 l_1^2 & m_2 a_2 l_1 \, cos(\theta_3 - \theta_2) \\ m_2 a_2 l_1 \, cos(\theta_2 - \theta_1) & I_2 + m_2 a_2^2 \end{bmatrix} \begin{bmatrix} \ddot{\theta}_2 \\ \ddot{\theta}_3 \end{bmatrix}$$
$$+ \begin{bmatrix} 0 & -m_2 a_2 l_1 \, sin(\theta_2 - \theta_1)\dot{\theta}_2 \\ m_2 a_2 l_1 \, sin(\theta_2 - \theta_1)\dot{\theta}_1 & 0 \end{bmatrix} \begin{bmatrix} \dot{\theta}_2 \\ \dot{\theta}_3 \end{bmatrix} \tag{8}$$
$$+ \begin{bmatrix} (m_1 a_1 + m_2 l_1) g \, sin\theta_1 / \theta_1 & 0 \\ 0 & m_2 a_2 g \, sin\theta_2 / \theta_2 \end{bmatrix} \begin{bmatrix} \theta_1 \\ \theta_2 \end{bmatrix} = 0.$$

We assume that the collision of the swing leg with the ground occurs plastically (the translational velocity at the tip of the swing leg becomes zero) and that there is a sufficient friction between the tip and the ground surface to prevent slippage. The angular velocities of the links after the collision are derived from conservation laws of momentum and angular momentum. They are calculated from Eq. (7) by putting $\tau = 0$.

To investigate the self-excited biped locomotion, a set of basic equations of (6), (7), and (8) were numerically solved based on the fourth-order Runge-Kutta method. The standard values of the link parameters used in the calculation are shown in Table 1. The values of mass and moment of inertia were calculated assuming uniform mass distribution along the link. Since the magnitude of the damping coefficient scarcely influences the biped gait, $\gamma_3 = 0.15 \, \text{Nms/rad}$ was used in the calculation.

		Link1	Link2	Link3
m_i	mass [kg]	4.0	2.0	2.0
I_i	length [kgm2]	0.21	0.027	0.027
l_i	Moment of inertia [m]	0.80	0.40	0.40
a_i	Offset of mass center [m]	0.40	0.20	0.20

Table 1. Link Parameter Values Used for Simulation Study (Ono, K. et al, 2001).

2.3 Simulation Results and Characteristics of Self-Excited Walking
In this simulation, we assumed that the support leg is kept straight due to internal torque during the first and second phases. To check whether the support leg can be lept straight by the passive knee stopper, the internal torque at the knee of the two-DOF support leg model was inversely calculated by using the calculated stable biped locomotion. Fig.4 plots the angular displacement of $\theta_1 - \pi$, θ_2, and θ_3 and the internal torques at the knees of the support and swing legs, which are calculated from θ_1, θ_2, and θ_3 based on the inverse dynamic analysis. The torque curve at $\phi_{off} = \theta_1 - \theta_2 \leq 0$. If the knee torque is negative, the reaction torque exists at the knee stpooer so that the support leg can be regarded as a single-DOF link. We observe that at the beginning of the first phase, the knee torque of the support leg becomes positive for a short time of less than 0.1 s.

Then, we calculated the knee torque of the support leg by assuming an offset angle of $\phi_{off} = \theta_2 - \theta_3 = 2$ degrees at the knee stopper. The calculated result is also shown in Fig.4. We note that the knee torque of the support leg shifts downward and changes to a negative value during the entire period. Moreover, it is seen from the negative knee torque of the swing leg that the swing leg can be kept straight during the second phase.

In the numerical sumulation, steady biped locomotion can be obtained as a limit cycle for the feedback gain value in a range of 4.8 Nm/rad $\leq k \leq$ 7.5 Nm/rad. When k is smaller than 4.8 Nm/rad, the initial step length gradually decreases and the biped mechanism falls down forward. When k is larger than 7.5 Nm/rad, the step changes irregularly and the biped mechanism falls down backwards because the swing leg is raised too high. Fig.5 shows the walking period, average velocity, and efficiency as a function of feedback gain k. The efficiency is defined as the ratio of average walking velocity to average input power, where the average input power is given by

$$P = \frac{1}{t_4 - t_0} \int\limits_{t=t_0}^{t=t_4} \left| \dot{\theta}_2 T_2 \right| dt \, . \tag{9}$$
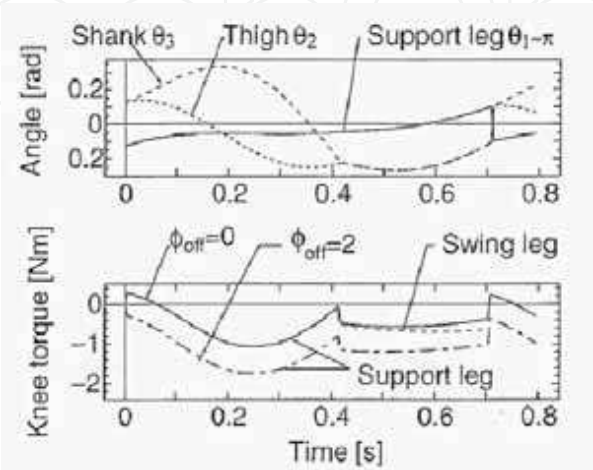

Fig.4. Motion of legs and internal torque at knee during one step (Ono, K. et al, 2001).
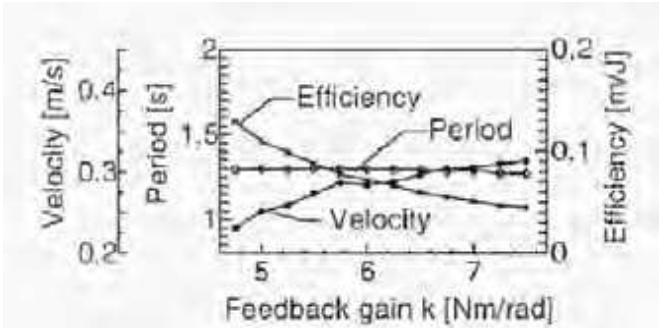

Fig.5. Effect of feedback gain on walking period, velocity, and efficiency (Ono, K. et al, 2001).

We note from this figure that the walking period shows an almost constant value of 1.3 s at any k value. This is because the self-excited biped locomotion is a natural motion inherent in the biped system. On the other hand, the average velocity increases gradually because of the increase in step length. However, the efficiency decreases with an increase in the feedback gain k because the average input power increases more rapidly with an increase in k. It is worthy to note that the average input power to generate biped locomotion with a velocity of 0.28 m/s is only about 4 W (=0.28/0.07) at k = 6.0 Nm/rad. If the additional movement of 0.6 m by feet during one period of 1.3 s is taken into account, the natural walking velocity becomes 2.7 km/h. the natural walking period of an adult with a 0.9 m leg height is 1.3 s (Yang 1994). Thus, it can be said that the calculated results of the walking period and velocity are comparable with the natural walking of an adult with a 0.8 leg height.

Validity of the self-excited walking stated above was confirmed experimentally (Ono, K., 2001). Extensions of the self-excited walking to a biped with feet and bent knee walking mode are described in (Ono, K., 2004) and (Kaneko, Y. & Ono K., 2006), respectively.

3. Energy-Efficient Trajectory Planning for Biped Walking Robot

In this section, we aim at realizing a energy-efficient walking of biped with actuators similar to a passive dynamic walking. We suggested optimal trajectory planning method based on a function approximation method, and applied for a biped walking robot analytically. We obtained the solutions which made the square integral value of input torque minimum. Until this point, we clarified the application of optimal trajectory planning method for biped walking robots, but they did not constrain the clearance between toe and ground at intermediate time of one period. As is generally known, it is necessary to give the clearance between toe and ground in the intermediate time of one step period. However, because there is the redundant degree of freedom by only constraining the clearance with equality state constraint, the solutions of undesired postures may be obtained. Therefore we suggest the optimal trajectory planning method with inequality state constraint that can restrict the joint angles to the desired range in a certain time. Concretely, we use inequality state constraint in the intermediate time and restrict the range of joint angles and may obtain a better solution which is desirable posture in the intermediate time.

With this method, we calculate optimal walking gait for biped with upper body mass. This model is attached the same masses to the support leg and swing leg in forward direction. And we examine the influence of installation position of the upper body mass.

And We perform a walking experiment by a prototype robot to inspect the effectiveness of this method. At first, in order to realize a stable walking, we attach a sensor at a sole to measure the time of grounding and compensate the error between reference trajectory and experimental trajectory. And, we install adjustment masses to revise parameters of the prototype robot. Furthermore, we use "Specific Cost" which shows energy consumption per unit mass and per unit movement velocity for evaluation of energy efficiency in section 4. By comparing the data of the other robots with this method, we show that our robot walks more efficiently than the other robots which use geared motors.

3.1 Analytical Model of Biped Walking Robot and Kinetic Process

3.1.1 Analytical Model and Kinetic Process

Fig.6 shows the three link biped model used in this research. Link 1 is the support, link 2 is the thigh, and link 3 is the shank. This model has upper body masses which is the same masses attached to the support leg and swing leg in forward direction. Table.3 shows the link parameters used in this analysis.

Table.2 shows symbols used in this paper (Hase, T.; Huang, Q. & Ono, K., 2006).

One step period is from Posture 1 to Posture 4 shown in Fig.7. State variables of Posture 4 are same as one of Posture 1. When it changes from Posture 3 to Posture 4, a collision between toe and ground happens, and link parameters exchange. In Posture 3, the swing leg collides with the ground, and becomes the support leg and the support leg leaves from the ground and comes back to Posture 4 (Posture 1). Leg exchange is performed by perfectly inelastic collision momentarily.

Symbols	Description
m_i	i-th link mass
I_i	i-th link moment of inertia
l_i	i-th link length
a_i	Length between i-th joint and i-th link COG
b_i	Length between $(i+1)$-th joint and i-th link COG
m_d	Upper body mass
d	Length between upper body mass and hip joint
θ_i	i-th link absolute angle
α_i	Offset angle between i-th link and i-th link COG from joint i
β_i	Offset angle between i-th link and i-th link COG from joint $(i+1)$
x_i	x-coordinate of i-th link COG
y_i	y-coordinate of i-th link COG
g	Acceleration of gravity
u_i	i-th joint input torque
J	Performance function
ζ_i	Dummy variable used for inequality constraint
δ_i	Clearance between toe and ground
$\boldsymbol{p}_i$	i-th coefficient vector of basis function
$\boldsymbol{h}_i$	i-th basis function
T	Period of one step
S	Length of ste

Table 2. Symbols used in this section (Hase T. & Huang, Q., 2005)
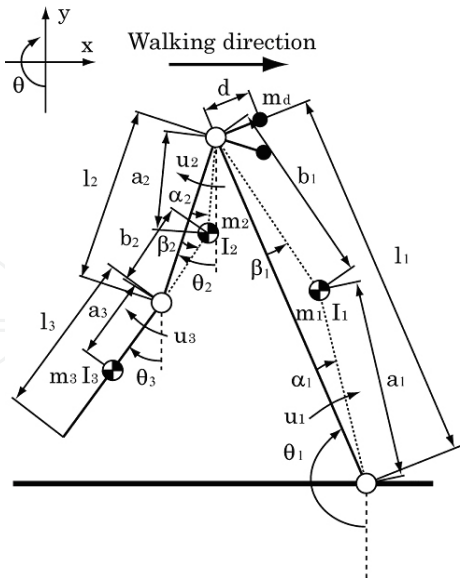
Fig.6. 3 link model with upper body mass (Hase T. & Huang, Q., 2005).

		Link1	Link2	Link3
m_i	[kg]	4.2	1.2	1.2
I_i	[kgm²]	0.127	0.029	0.029
l_i	[m]	0.60	0.30	0.30
a_i	[m]	0.339	0.115	0.125

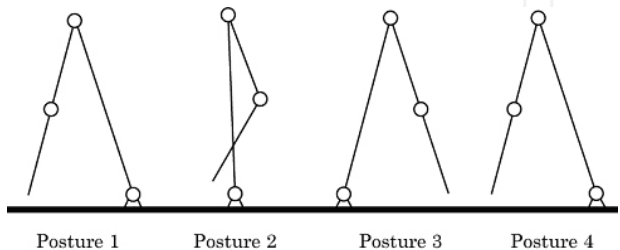Table 3. Link parameters (Hase T. & Huang, Q., 2005).

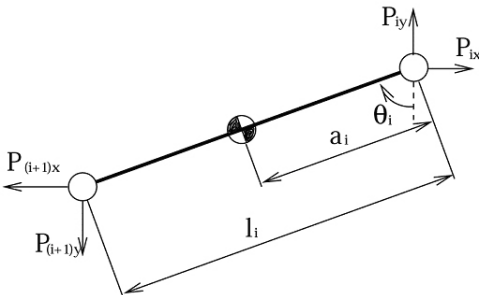Fig.7. Process of one step walking (Hase T. & Huang, Q., 2005).

Fig.8. Impulse for *i*-th link (Hase T. & Huang, Q., 2005).

3.1.2 Dynamic Equations and Analysis of Collision between Toe and Ground

By the analytical model shown in Fig.6, dynamic equations are lead as follows. We assumed that there is no friction in each joint.

$$M(\theta)\ddot{\theta} + C(\theta)\dot{\theta}^2 + K(\theta) = u \tag{10}$$

When collision between toe and ground occurs, it is assumed that a momentum and angular momentum of each link are conserved. Leg exchange happens shown as Fig.7.

Fig.8 shows impulse for *i*-th link. "v_{ix}", "v_{iy}" is x, y ingredient of translation velocity of a center of gravity of each link. "+" indicates the state just after the swing leg collides with the ground, and "-" indicates the state just before that.

Using the conservation law of momentum and angular momentum, following equations work out.

$$\begin{cases} m_i(v_{ix}^+ - v_{ix}^-) = P_{ix} - P_{(i+1)x} \\ m_i(v_{iy}^+ - v_{iy}^-) = P_{iy} - P_{(i+1)y} \\ I_i(\theta_i^+ - \theta_i^-) = a_i \times P_i + (l_i - a_i) \times P_{i+1} \end{cases} \tag{11}$$

When Eq.(10) are organized, angular velocity just before and after collision are as follows.

$$M(\theta)\dot{\theta}^+ = H(\theta)\dot{\theta}^- \tag{12}$$

Matrices in Eq.(10), (12) are written in (Ono, K. & Liu, R., 2002).

3.2 Optimal Trajectory Planning Method with Inequality Constraint

3.2.1 Conventional Optimal Trajectory Planning Method (Ono, K. & Liu, R., 2002)

We apply the function approximation method to express the joint angle trajectory by Hermite polynomial function set. Then the optimal trajectory planning problem is converted into the parameter optimization problem of the coefficients of the basis function. The joint angle trajectory is expressed as follows:

$$\theta(p,t) = h(t)^T p \tag{13}$$

where $h(t)$ is the Hermite basis function vector and p is the coefficient vector of the basis function. Here, the coefficient vector is the boundary state variable vector.

The total constraint conditions and the performance index which are function of p are expressed as follows:

$$C(p) = 0 \tag{14}$$

$$J = J(p) \tag{15}$$

then, we obtain the solution which make Eq.(15) minimum while Eq.(14) is satisfied.

The approximated solution p_{k+1} in the (k+1)-th step of Eq.(14) is solved by Newton-Raphson iteration method in the following form:

$$\frac{\partial C(p_k)}{\partial p}\Delta p = -C(p_k)$$
$$(\Delta p = p_{k+1} - p_k) \tag{16}$$

In Eq.(16), the unknown variable number is far more than the equation number. Therefore, the number of the solutions which satisfy Eq.(14) is infinite. A particular solution is solved using the singular value decomposition (SVD).

Then, the general solutions Δp become as follows:

$$\Delta p = \Delta p_0 - B q \tag{17}$$

p_0 is a particular solution. B is solved by using the SVD method, and q is the null-space vector to be determined from the J minimum condition as follows:

$$\frac{\partial J}{\partial q} = \frac{\partial J}{\partial p}B = 0 \tag{18}$$

In order to solve q to satisfy Eq.(18), we use Newton-Raphson iteration method. The second order partial differentiation of J with respect to q is calculated as follows:

$$\frac{\partial^2 J}{\partial q^2} = B^T \frac{\partial^2 J}{\partial p^2}B \tag{19}$$

Then, we obtain p from q and obtain the optimal solution.

3.2.2 Introducing the Inequality Constraint

Conventionally, we used only equality constraint at the beginning, middle and ending time for a biped walking robot. But there is such a case that the joint angle should pass the desirable ranges without being restricted precisely. In that case, the better solution will be obtained when the joint angle is restricted with inequality constraint than equality constraint. When we use inequality constraint, we convert Eq.(14) into follow equations with dummy variables.
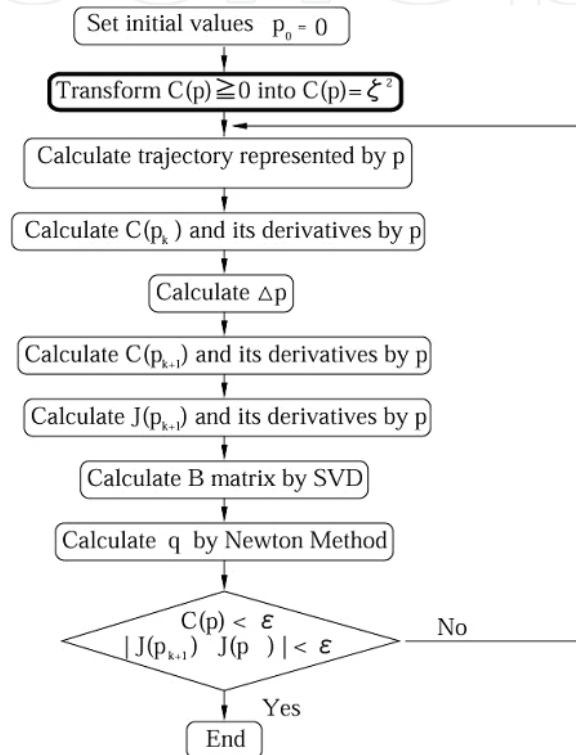

Fig.9. Flowchart of this algorism   (Hase T. & Huang, Q., 2005).

$$C(p) \geq 0 \quad \Rightarrow \quad C(p) = \varsigma^2$$
$$C(p) \leq 0 \quad \Rightarrow \quad C(p) = -\varsigma^2 \tag{20}$$

Then, we use the dummy variables as optimization parameters.

For example, if you restrict the state variable of joint angle at boundary time t_i as follows:

$$\theta(t_i) \geq 0 \tag{21}$$

Then, the dummy variable introduced as follows:

$$\theta(t_i) = \varsigma^2 \tag{22}$$

The state variables at boundary time t_i are expressed as j-th optimization parameter p_j as follows:

$$\theta(t_i) = p_j \tag{23}$$

Here, Eq.(22) and Eq.(23) are organized as follows:

$$p_j = \varsigma^2 \tag{24}$$

Then, we convert p_j into ς^2 in a coefficient parameter of the performance index, basis function, and other constraints. Optimization calculation is performed with respect to ς and other parameters (not p_j). Fig.9 shows the flowchart of this algorithm.

3.3 Application for Biped Walking Robot

3.3.1 Performance Function
In order to obtain a natural walking solution with the lowest input torque, the performance index in this paper is defined as the sum of the integration of square input torque as follows:

$$J = \sum_{i=1}^{3} k_i \int_0^T u_i^2(t)dt \tag{25}$$

where k_i is the weighting factor corresponding to joint i, and u_i is the input torque at joint i. When joint i is passive joint, we relatively make k_i larger and bring the passive joint torque close to 0.

3.3.2 The Results of Using Equality Constraint at Beginning and Ending Time
At first, the period T of one step and the length of the step S are determined. The beginning and ending posture is that both legs become straight. This posture is determined when the length of the step is determined.
Fig.10 and Fig.11 show stick figure of trajectory, joint input torque, angular velocity, and clearance between toe and ground at T=0.60[s], S=0.15[m].
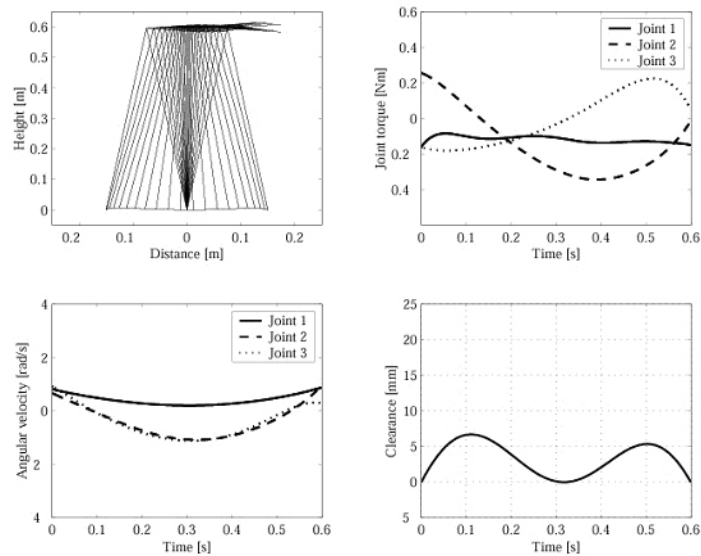
Fig.10. The result of using equality constraint at beginning and ending time (S=0.150[m] T=0.60[s]) (Hase T. & Huang, Q., 2005).
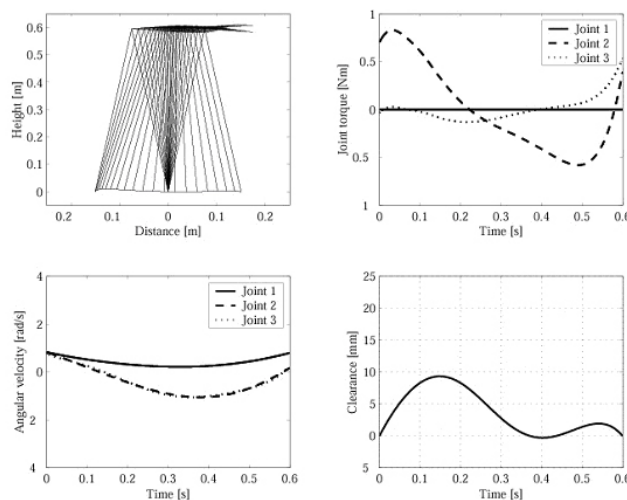
Fig.11. The result of using equality constraint at beginning and ending time (u_1 =0, S=0.150[m], T=0.60[s]) (Hase T. & Huang, Q., 2005).

3.3.3 The Results of Using Inequality Constraint at Intermediate Time

From the result of preceding section, there is the moment when toe comes in contact with ground. There is not utility in this result.

Then, we give the clearance (δ) between toe and ground by constraining the posture at intermediate time (0.5T). The constraint is expressed as follows:

$$\delta = -l_1 \, cos\theta_1 \left(0.5T\right) - l_2 \, cos\theta_2 \left(0.5T\right) - l_3 \, cos\theta_3 \left(0.5T\right) \qquad (26)$$

This constraint has three variables and becomes redundant. It is desirable that the joint angles come to the following range so that it is natural walking.

$$\theta_2 \left(0.5T\right) \leq 0$$
$$\theta_3 \left(0.5T\right) \geq 0 \qquad (27)$$

These inequality constraints are converted into following equality constraints.

$$\theta_2 \left(0.5T\right) = -\zeta_1^2$$
$$\theta_3 \left(0.5T\right) = \zeta_2^2 \qquad (28)$$

Figs.12 and 13 show the results of δ =20[mm]. These results show that clearance condition is satisfied.

3.3.4 A Change of the Evaluation Function for a Change of a Period

Figs.14 and 15 show the changes of performance function J for change of period T. Conventionally, we constrained the swing leg posture at intermediate time with equality constraint. These graphs compare this method (inequality) with a conventional method (equality), and the performance function J by this method is smaller than that of a conventional method. They have local minimum solutions between 0.6s from 0.5s.
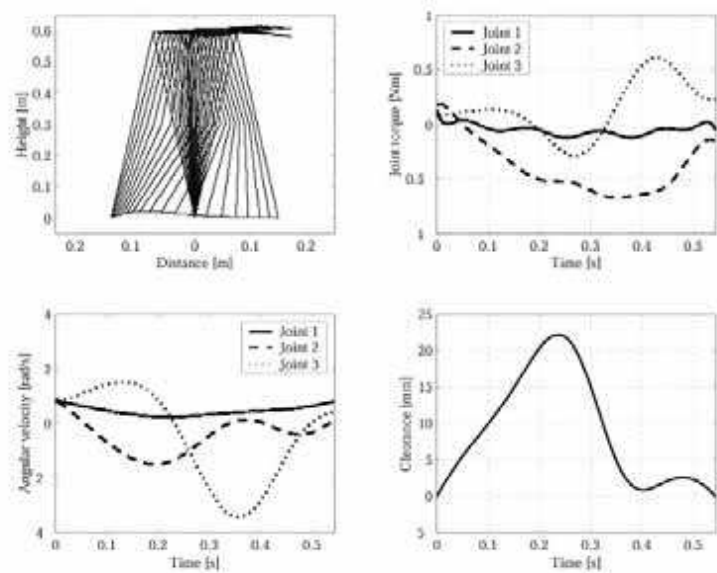
Fig.12. The result of using inequality constraint at intermediate time (δ =20[mm], S=0.150[m], T=0.55[s]) (Hase T. & Huang, Q., 2005).
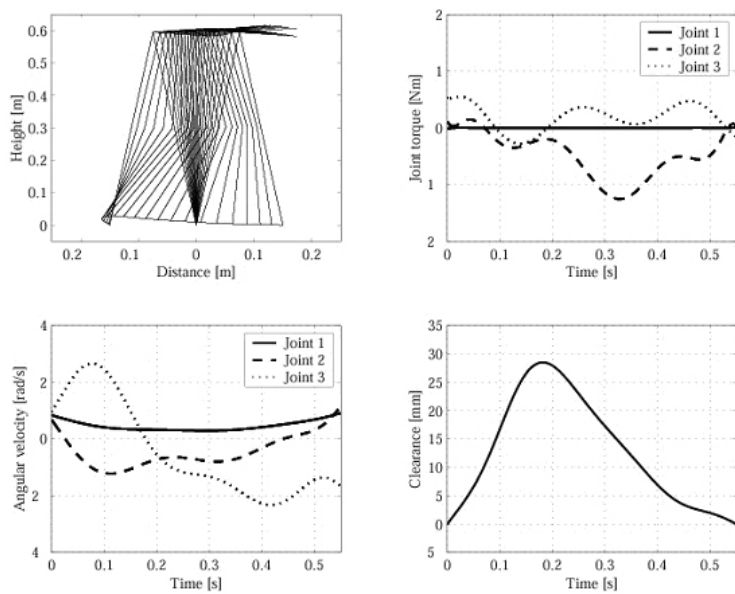

Fig.13. The result of using inequality constraint at intermediate time (u_1 =0, δ =20[mm], S=0.150[m], T=0.55[s]) (Hase T. & Huang, Q., 2005).

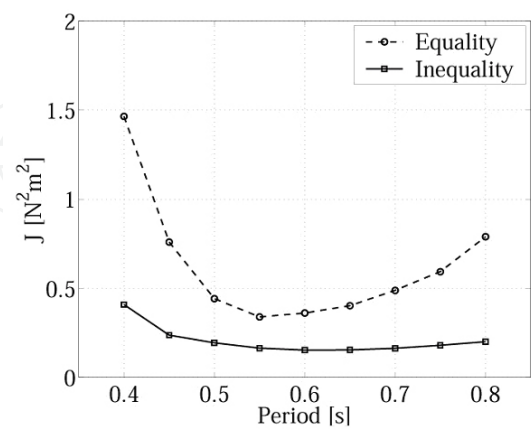Fig.14. Change of performance function J for change of period T (δ =20[mm], S=0.15[m]) (Hase T. & Huang, Q., 2005).
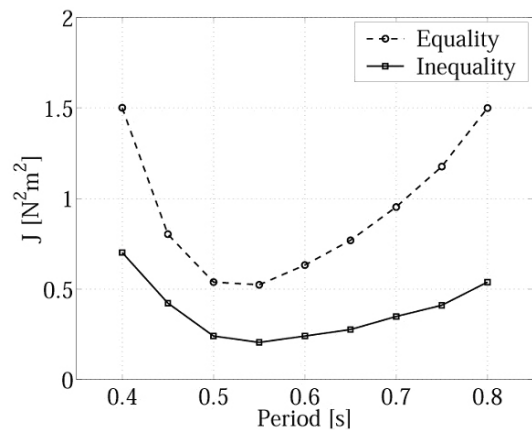

Fig.15. Change of performance function J for change of period T (u_1 =0, δ =20[mm], S=0.15[m]) (Hase T. & Huang, Q., 2005).

3.3.5 The Influence of Installation position of the upper body mass

Fig.16 shows influence of installation position of the upper body mass. When u_1 is 0, the input becomes larger as the installation position becomes longer. When u_0 is 0, there is an optimal installation position at 80mm.

3.4. Walking Experiment for Energy-Efficient Trajectory Planning

3.4.1 Hardware

Fig.17 shows the summary of the prototype robot. This robot has three legs to constraint the motion of roll direction. Hip joint and knee joint have actuators. These actuators are DC motors with gear reducer. They are controlled by motor drivers. Table.4 shows the parameters of the prototype robot.
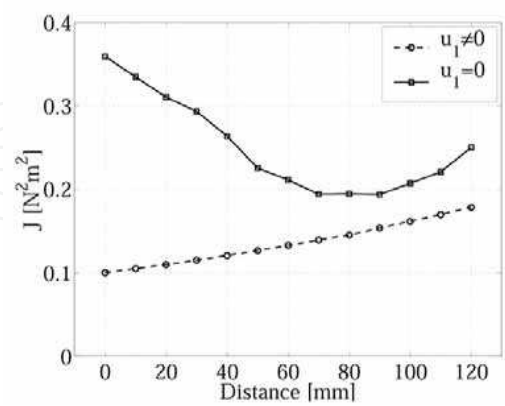
Fig.16. The influence of installation position of the upper body mass (δ =20[mm], T=0.55[s]) (Hase T. & Huang, Q., 2005).

Fig.17. Prototype robot   (Hase T. & Huang, Q., 2005).

	Inner		Outer	
	Thigh	Shank	Thigh	Shank
m [kg]	3.02	1.22	2.92	1.20
I [kgm²]	0.027	0.015	0.031	0.017
$_l$[m]	0.30	0.30	0.30	0.30
a [m]	0.10	0.12	0.13	0.13

Table 4. Link parameters   (Hase T. & Huang, Q., 2005).

3.4.2 Software

We performed an optimization calculation in offline beforehand and save the data of relative joint angle trajectory. It is the best that robot controlled with feed forward control of optimal torque. But it is difficult to measure the parameters of experimental robot and collision between toe and ground precisely. Therefore, we used PD feedback control for each joint and let the experimental trajectory follow the optimal trajectory.

In the experiment, the timing of a landing does not agree with the analysis and the delay occurs for optimal trajectory. Then, we attached a touch sensor at a sole and the input of the next period starts when a sensor becomes on. The robot keeps the ending posture until the toe lands.

The analysis model has only three links and assumed the support leg to be one link. We attached stoppers to knee joints and fixed it by pushing it to stoppers with motors when the leg becomes support leg.

3.4.3 The Results of Walking Experiment

Figs.18 and 19 show the results of eight steps of walking experiment. Fig.18 is relative joint angle. It has delay, but almost follows the optimal trajectory. Because we used PD feed back control in order to cancel model simplifications (no backlash, friction at joints, perfect inelastic collision between toe and ground). Fig.19 shows the PD feedback input torque. When the legs collide with the ground, they vibrate and PD feedback input becomes larger.
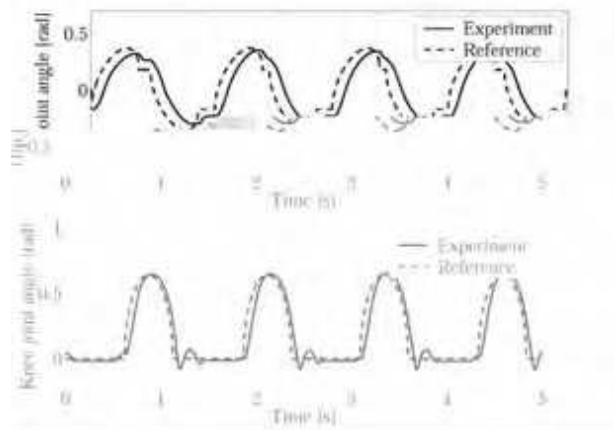

Fig.18. Joint angle trajectory   (Hase T. & Huang, Q., 2005).

4. Energy Efficiency

Energy efficiency of walking can be evaluated with Specific Cost "C" (the energy consumed per unit mass and per transport velocity) as follows:

$$C = \frac{P}{mgv} \tag{29}$$

Here, P is the energy consumed per unit of time [W], m is mass[kg], v is transport velocity[m/s].

In the case of the self-excited mechanism, there is one type of Specific Cost C_{mt} that calculated by the simulation results in section 2.3. In this case, C_{mt} is obtained with the

mechanical work energy (4W) and walking velocity (0.28m/s) for the 8kg weight of the robot model. Then, C_{mt} become about 0.18.
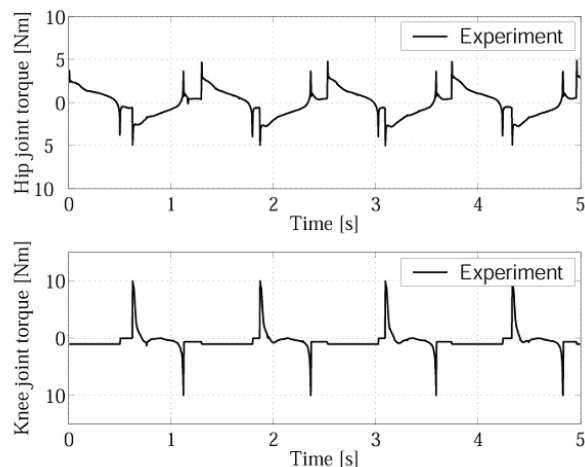

Fig.19. Joint input torque (Hase T. & Huang, Q., 2005).

And then, in the case of the optimal trajectory planning, there are two types of Specific Cost (C_{et}, C_{mt}). C_{et} is obtained with the energy that consumed at the motors (11.7W), microcomputer, and sensors (5W). C_{et} become 0.68. C_{mt} is obtained with the mechanical work energy (8.8W). Then, C_{mt} become 0.36. Table.5 shows C_{et} and C_{mt} of some types of biped walking robots (Collins, S. H. & Ruina A., 2005).

	C_{et}	C_{mt}	Actuator
Honda's Asimo	3.2	1.6	
Our Robot (Self-Excited Machanism)	-	0.18	Geared motor
Our Robot (Optimal trajiectry planning)	0.68	0.36	
T.U.Delft's Denise	5.3	0.08	Pneumatic McKibben muscle
MIT's Spring Flamingo Comell's Biped	2.8	0.07	Series elastic actuator
	0.2	0.055	Push-off actuator
McGeer's Dynamite	-	0.04	

Table 5. Specific cost of transport and mechanical energy efficiency of biped walking robots.

As our robots uses gears of large reduction ratio, the energy consumption by friction grows large, and Specific Cost grows larger than the other robots which used the mechanism of passive dynamic walking. However, it is very smaller than the other type robot using the gears of large reduction ratio.

5. Conclusion

In this chapter, we introduced the researches on energy-efficient walking of the biped robot for level ground form two viewpoints, one is semi-passive dynamic walking with only hip actuator using self-excited mechanism, another is active walking with actuators using optimal trajectory planning. We can make the conclusions as follow.

In the case of energy-efficient walking using the self-excited mechanism:

1. To develop an efficient control method of natural biped locomotion, the self-excitation control of asymmetry stiffness type was applied to the biped mechanism to generate natural walking.
2. In a two-DOF swing leg whose thigh and shank are connected by a passive knee joint, the input torque at the hip joint can generate a walking gait of the swing leg and can increase the swing amplitude and its kinetic energy.
3. From the simulation for a biped mechanism whose leg is as tall as 0.8 m (similar to a standard adult), the walking period is 1.3s and walking velocity 0.28m/s at an average input power of 4W. According to the Specific Cost data comparing with the other types of biped walking robots, we showed that the energy-efficient walking is possible using the self-excited mechanism for biped locomotion.

In the case of energy-efficient walking using the optimal trajectory planning:

1. We proposed optimal trajectory planning method based on a function approximation method, and applied for a biped walking robot analytically. And in order to avoid the solutions of undesired postures when constrain the clearance between toe and ground at intermediate time of one period, we proposed an optimal trajectory planning method with inequality constraint, and applied it to a biped walking robot with upper body mass.

2. We performed a walking experiment by a prototype robot to inspect the effectiveness of this method. In the walking experiment, we realized the stable walking. One step period was 0.6s, and walking velocity was 0.3m/s.

3. We showed the energy-efficient walking using the proposed optimal trajectory planning method for biped locomotion by comparing Specific Cost of other robots with geared motors.

8. References

McGeer, T. (1990). Passive Dynamic Walking, *International Journal of Robotics Research*, Vol.9, pp.62-82

Collins, S. H. & Ruina A. (2005). A Bipedal Walking robot with efficient and human-like gait, *Proceedings of IEEE International Conference of Robotics and Automation*, Barcelona, Spain, Biped Locomotion I, CD-ROM No.1935

Wisse, M. & Frankenhuyzen, J. van (2003). Design and construction of MIKE; a 2d autonomous biped based on passive dynamic walking, *Proceedings of Conference of Adaptive Motion of Animals and Machines*, Kyoto, Japan, Analysis & Control of Bipedal Locomotion, CD-ROM No.WeP-I-1

Ono, K. & Okada, T. (1994). Self-excited vibratory actuator (1st report: Analysis of two-degree-of-freedom self-excited systems), *Transactions of the JSME(C)*, Vol.60, No.577, pp.92-99 (in Japanese)

Ono, K.; Takahashi, R.; Imadu, A. & Shimada, T. (2001). Self-excited walking of a biped mechanism, *International Journal of Robotics Research*, Vol.20, No.12, pp.953-966

Ono, K.; Furuichi, T. & Takahashi, R. (2004). Self-Excited Walking with Feet, *International Journal of Robotics Research*, Vol.23, No.1, pp.55-68

Kaneko, Y. & Ono K. (2006). Study of Self-Excited Biped Mechanism with Bending Knee, *Transactions of the Japan Society of Mechanical Engineers*, Series C, Vol.72, No.714, pp.416-434 (in Japanese)

Osuka, K.; Sugimoto Y. & Sugie T. (2004). Stabilization of Semi-Passive Dynamic Walking based on Delayed Feedback Control, *Journal of the Robotics Society of Japan*, Vol.22, No.1, pp.130-139 (in Japanese)

Asano, F.; Luo, Z.-W. & Yamakita, M. (2004). Gait Generation and Control for Biped Robots Based on Passive Dynamic Walking, Journal of the Robotics Society of Japan, Vol.22, No.1, pp.130-139

Imadu, A. & Ono, K. (1998). Optimum Trajectory Planning Method for a System that Includes Passive Joints (1st Report, Proposal of a Function Approximation Method), *Transactions of the Japan Society of Mechanical Engineers*, Series C, Vol.64, No.618, pp.136-142 (in Japanese)

Ono, K. & Liu, R. (2001). An Optimal Walking Trajectory of Biped Mechanism (1st Report, Optimal Trajectory Planning Method and Gait Solutions Under Full-Actuated Condition), *Transactions of the Japan Society of Mechanical Engineers*, Series C, Vol.67, No.660, pp.207-214 (in Japanese)

Liu, R & Ono, K. (2001). An Optimal Trajectory of Biped Walking Mechanism (2nd Report, Effect of Under-Actuated Condition, No Knee Collision and Stride Length), *Transactions of the Japan Society of Mechanical Engineers*, Series C, Vol.67, No.661, pp.141-148 (in Japanese)

Ono, K. & Liu, R. (2002). Optimal Biped Walking Locomotion Solved by Trajectory Planning Method, Transactions of the ASME, *Journal of Dynamic Systems, Measurement and Control*, Vol.124, pp.554-565

Peng, C. & Ono K. (2003). Numerical Analysis of Energy-Efficient Walking Gait with Flexed Knee for a Four-DOF Planar Biped Model, *JSME International Journal*, Series C, Vol.46, No.4, pp.1346-1355

Hase T. & Huang, Q. (2005). Optimal Trajectory Planning Method for Biped Walking Robot based on Inequality State Constraint, *Proceedings. of 36th International Symposium on Robotics*, Biomechanical Robots, CD-ROM, WE413, Tokyo, Japan

Hase, T.; Huang, Q. & Ono, K. (2006). An Optimal Walking Trajectory of Biped Mechanism (3rd Report, Analysis of Upper Body Mass Model under Inequality State Constraint and Experimental Verification), *Transactions of the Japan Society of Mechanical Engineers*, Series C, Vol.72, No.721, pp.2845-2852 (in Japanese)

Huang, Q.. & Hase, T. (2006). Energy-Efficient Trajectory Planning for Biped walking Robot, *Proceedings. of the 2006 IEEE International Conference on Robotics and Biomimetics*, pp.648-653, Kunming, China

Humanoid Robots: New Developments

Edited by Armando Carlos de Pina Filho

For many years, the human being has been trying, in all ways, to recreate the complex mechanisms that form the human body. Such task is extremely complicated and the results are not totally satisfactory. However, with increasing technological advances based on theoretical and experimental researches, man gets, in a way, to copy or to imitate some systems of the human body. These researches not only intended to create humanoid robots, great part of them constituting autonomous systems, but also, in some way, to offer a higher knowledge of the systems that form the human body, objectifying possible applications in the technology of rehabilitation of human beings, gathering in a whole studies related not only to Robotics, but also to Biomechanics, Biomimmetics, Cybernetics, among other areas. This book presents a series of researches inspired by this ideal, carried through by various researchers worldwide, looking for to analyze and to discuss diverse subjects related to humanoid robots. The presented contributions explore aspects about robotic hands, learning, language, vision and locomotion.

How to reference

In order to correctly reference this scholarly work, feel free to copy and paste the following:

Qingjiu Huang and Kyosuke Ono (2007). Energy-Efficient Walking for Biped Robot Using Self-Excited Mechanism and Optimal Trajectory Planning, Humanoid Robots: New Developments, Armando Carlos de Pina Filho (Ed.), ISBN: 978-3-902613-00-4, InTech, Available from:
http://www.intechopen.com/books/humanoid_robots_new_developments/energy-efficient_walking_for_biped_robot_using_self-excited_mechanism_and_optimal_trajectory_plannin

INTECH
open science | open minds